8032 *Biochemistry* **2009,** *48,* 8032–8043
DOI: 10.1021/bi9010013

BIOCHEMISTRY
including biophysical chemistry & molecular biology
Article

The Amino Acid Motif L/IIxxFE Defines a Novel Actin-Binding Sequence in PDZ-RhoGEF[†]

Jayashree Banerjee, Christopher C. Fischer, and Philip B. Wedegaertner*

Department of Biochemistry and Molecular Biology, Thomas Jefferson University, Philadelphia, Pennsylvania 19107

Received June 14, 2009; Revised Manuscript Received July 20, 2009

ABSTRACT: PDZ-RhoGEF is a member of the regulator family of G protein signaling (RGS) domain-containing RhoGEFs (RGS-RhoGEFs) that link activated heterotrimeric G protein α subunits of the G12 family to activation of the small GTPase RhoA. Unique among the RGS-RhoGEFs, PDZ-RhoGEF contains a short sequence that localizes the protein to the actin cytoskeleton. In this report, we demonstrate that the actin-binding domain, located between amino acids 561 and 585, directly binds to F-actin in vitro. Extensive mutagenesis identifies isoleucine 568, isoleucine 569, phenylalanine 572, and glutamic acid 573 as being necessary for binding to actin and for colocalization with the actin cytoskeleton in cells. These results define a novel actin-binding sequence in PDZ-RhoGEF with a critical amino acid motif of IIxxFE. Moreover, sequence analysis identifies a similar actin-binding motif in the N-terminus of the RhoGEF frabin, and as with PDZ-RhoGEF, mutagenesis and actin interaction experiments demonstrate an LIxxFE motif, consisting of the key amino acids leucine 23, isoleucine 24, phenylalanine 27, and glutamic acid 28. Taken together, results with PDZ-RhoGEF and frabin identify a novel actin-binding sequence. Lastly, inducible dimerization of the actin-binding region of PDZ-RhoGEF revealed a dimerization-dependent actin bundling activity in vitro. PDZ-RhoGEF exists in cells as a dimer, raising the possibility that PDZ-RhoGEF could influence actin structure in a manner independent of its ability to activate RhoA.

Rho family GTPases are members of the Ras superfamily of monomeric G proteins (*1*). The Rho family comprises six small GTPase subfamilies, including Rho, Rac, Cdc42, Rnd, RhoBTB, and RhoT/Miro (*2*). Of these, the most well-studied members include Rho (A, B, and C), Rac (1 and 2), and Cdc42 proteins. Their roles in cell regulation include modulation of cytoskeletal structure, motility, cell division, gene transcription, vesicular transport, and various enzymatic activities. As key regulators of the actin cytoskeleton, in fibroblasts, RhoA induces the formation of actin stress fibers and focal adhesions, Rac1 stimulates the protrusion of lamellipodia and membrane ruffles, and Cdc42 promotes extension of filopodia and actin microspikes (*3*−*5*). Rho GTPases are found in all eukaryotic cells, and so far, 22 mammalian genes encoding Rho GTPases have been described (*6*).

Rho GTPases act as molecular switches, cycling between an active GTP-bound state and an inactive GDP-bound state. They are converted from an inactive (GDP-bound) state to an active state (GTP-bound) by guanine nucleotide exchange factors (GEFs)[1] that function downstream of ligand-bound integrins, growth factor receptors, and heterotrimeric G protein-coupled receptors (GPCRs). The RhoGEFs are the best-understood regulators of Rho activation in response to upstream stimuli (*7*), and so far, ∼70 RhoGEFs have been identified in the human genome (*8*, *9*). The RhoGEFs are characterized by tandem Dbl homology (DH) and pleckstrin homology (PH) domains. In addition to the signature DH−PH domains, the RhoGEFs also contain a variety of other signaling domains that mediate interaction with numerous proteins resulting in a multitude of events.

Unique among the large family of RhoGEFs is a subfamily that contains a regulator of the G protein signaling (RGS) domain and is hence named RGS-RhoGEF. The RGS-RhoGEFs in mammals consist of p115-RhoGEF, PDZ-RhoGEF (PRG), and leukemia-associated Rho-GEF (LARG). These form an important group of proteins as they provide a direct link for activation of RhoA by cell surface receptors coupled to heterotrimeric G proteins. Further, these exchange factors are specific for RhoA and do not activate Rac or Cdc42 (*10*−*14*). In addition to their RGS, DH, and PH domains, which are characteristic of all three mammalian RhoGEFs, PRG and LARG contain an N-terminal PDZ domain.

PDZ domains of PRG and LARG have been shown to interact with plexins B1 and B2, LPA receptors (LPA_1 and LPA_2), insulin-like growth factor (IGF-1) receptor, and light chain 2 (LC2) of microtubule-associated protein (MAP) (*14*−*19*). Moreover, PRG and LARG are phosphorylated on tyrosine residues by focal adhesion kinase (FAK) in response to GPCR agonist stimulation of G proteins (*20*), and it has been shown that FAK, PRG, and ROCK II cooperate to induce Rho/ROCK II-dependent focal adhesion movement and trailing-edge retraction in response to LPA in fibroblasts (*21*). p115-RhoGEF, PRG, and LARG have also been shown to form homo- and hetero-oligomers, and the

[†]This work was supported by National Institutes of Health Grant GM62884 (P.B.W.).

*To whom correspondence should be addressed: Department of Biochemistry and Molecular Biology, Thomas Jefferson University, 233 S. 10th St., 839 BLSB, Philadelphia, PA 19107. Telephone: (215) 503-3137. Fax: (215) 923-2117. E-mail: P_Wedegaertner@mail.jci.tju.edu.

[1]Abbreviations: GEF, guanine nucleotide exchange factor; RGS, regulator of G protein signaling; PH, pleckstrin homology; DH, Dbl homology; PRG, PDZ-RhoGEF.

 Published on Web 07/20/2009

C-terminal regions of the proteins are involved in their oligomerization (*22*, *23*).

PDZ-RhoGEF (PRG), alternatively known as KIAA0380, ArhGEF11, or GTRAP48, is unique among the other RhoGEFs, LARG and p115Rho-GEF. While p115-RhoGEF and LARG are substantially activated by $G\alpha_{13}$, PRG displays little or no activation of its Rho exchange activity when combined with $G\alpha_{13}$ in vitro (*24*−*27*). PRG, a predominatly brain specific RhoGEF (*28*), is able to induce neurite retraction in Neuro 2a cells. It has been shown that PRG promotes cell rounding and an increase in the level of cortical actin in Swiss 3T3 cells (*12*), whereas p115-RhoGEF induces stress fibers but not cortical actin reorganization or cell rounding.

Previously, we demonstrated that PRG colocalizes with the actin cytoskeleton in cultured cells and binds to actin complexes in cell lysates through a unique 25-amino acid region (amino acids 561−585) that is located between the RGS and DH−PH domains of the protein (*29*). PRG mutants that fail to interact with actin displayed an enhanced Rho-dependent signaling compared to that of wild-type PRG. In the previous study, it was not determined whether PRG directly binds actin or whether the interaction with actin was mediated by other actin-binding proteins. Here, we now demonstrate that the actin-binding region of PRG directly binds F-actin in vitro. In addition, we further characterize the actin-binding region of PRG by point mutation analysis, immunofluorescence localization, co-immunoprecipitation, and actin cosedimentation assays. We have identified the importance of four specific amino acids (I^{567}, I^{568}, F^{573}, and E^{574}) in the actin-binding domain of PRG that are directly responsible for in vitro actin binding as well as in vivo colocalization with the actin cytoskeleton. Moreover, our studies demonstrate that a similar actin-binding motif exists in frabin, a RhoGEF that is not a member of the RGS-RhoGEF subfamily. Lastly, we report here that dimerization of the actin-binding region of PRG reveals an in vitro F-actin bundling activity.

MATERIALS AND METHODS

Plasmid Construction. The N-terminal Myc epitope (EQKLISEED)-tagged PRG and (Δ25)PRG in pCDNA3 have been described previously (*29*). Myc epitope-tagged frabin and GST-Dead FAB-PH1 frabin DNA (*30*) was kindly provided by Y. Takai (Osaka University Graduate School of Medicine, Suita, Japan).

GST(541−605)PRG and GST(541−605,Δ25)PRG were constructed by PCR amplification with Myc-PRG and Myc-(Δ25)-PRG as templates, respectively, and subcloning into EcoRI and SalI restriction sites of pGEX5X-1. Frabin(1−150)GFP was generated by PCR amplification using Myc-frabin as a template and subcloning into the EcoRI and SalI restriction sites of pEGFP-N1. Furthermore, GST(1−150)frabin was made by PCR amplification with GST-Dead FAB-PH1 frabin as a template and subcloning into EcoRI and SalI restriction sites of pGEX5X-1.

The Stratagene QuikChange site-directed mutagenesis kit (Stratagene, La Jolla, CA) was used to replace amino acids with alanine to create Myc(N567A)PRG, Myc(I568A)PRG, Myc-(I569A)PRG, Myc(Q570A)PRG, Myc(H571A)PRG, Myc-(F572A)PRG, Myc(E573A)PRG, Myc(N574A)PRG, and Myc(N575A)PRG using Myc-PRG as a template. GST(541−605,I568A)PRG, GST(541−605,I569A)PRG, GST(541−605, F572A)PRG, GST(541−605,E573A)PRG, and GST(541−605, N574A)PRG were obtained using GST(541−605)PRG as a template. Frabin(1−150,D22A)GFP, frabin(1−150,L23A)GFP, frabin(1−150,I24A)GFP, frabin(1−150,S25A)GFP, frabin(1−150,H26A)GFP, frabin(1−150,F27A)GFP, frabin(1−150,E28A)-GFP, frabin(1−150,G29A)GFP, and frabin(1−150,G30A)GFP were generated using frabin(1−150)GFP as a template, and GST(1−150,L23A)frabin, GST(1−150,I24A)frabin, GST(1−150, F27A)frabin, and GST(1−150,E28A)frabin were made using GST(1−150)frabin as a template.

FKBP from pC_4-F_v1E (Ariad Pharmaceuticals, Cambridge, MA) was amplified with forward and reverse primers containing a 5′ XhoI site and a 3′ NotI site for subcloning into GST(541−605)PRG to make GST(541−605)PRG-FKBP. The correct sequences of the mutants were confirmed by DNA sequencing of the entire open reading frame (Kimmel Cancer Center Nucleic Acid Facility, Philadelphia, PA).

Cell Culture and Transfection. COS-7 cells were propagated in DMEM (Mediatech, Herndon, VA) containing 10% fetal bovine serum and penicillin and streptomycin. Unless otherwise mentioned, cells were plated in six-well plates at a density of 7.0×10^5 cells/well and grown for 24 h before transfection. One microgram of total expression plasmid was transfected into the cells by using FuGENE 6 (Roche Diagnostics, Indianapolis, IN).

Immunofluorescence Microscopy. COS-7 cells were grown on coverslips in six-well plates and transfected with appropriate plasmids for 24 h. Fixation and staining have been described previously (*29*). Briefly, cells were fixed with 3.7% formaldehyde in phosphate-buffered saline (PBS) for 15 min, washed, and then incubated in blocking buffer containing 2.5% nonfat milk in a Tris-buffered saline (TBS)/1% Triton X-100 mixture. Cells were incubated with 1 μg/mL 9E10, anti-Myc mouse monoclonal antibody (Covance, Berkeley, CA) for 1 h, and then Alexa 594 goat anti-mouse secondary antibody (Molecular Probes, Eugene, OR) at a dilution of 1:250 for 45 min. For green fluorescent protein (GFP)-tagged mutants, incubation with antibodies was omitted. For the detection of actin, phalloidin conjugated to Alexa 488 or 594 (Molecular Probes) was used at a dilution of 1:100 for 45 min. Thereafter, coverslips were washed with a TBS/1% Triton X-100 mixture, rinsed in distilled water, and mounted on glass slides with 10 μL of Prolong Antifade Reagent (Molecular Probes).

Images were acquired using an Olympus BX-61 upright microscope with a 60 × 1.4 NA oil immersion objective and an ORCA-ER cooled charge-coupled device camera (Hamamatsu, Bridgewater, NJ) controlled by Slidebook version 4.0 (Intelligent Imaging Innovations, Denver, CO).

F-Actin Co-Immunoprecipitation Assay. COS-7 cells grown in 10 cm plates were transfected with 7 μg of the indicated constructs. Twenty-four hours after transfection, cells were washed twice with cold PBS and lysed using 500 μL of lysis buffer as described previously (*29*). Briefly, cells were lysed for 45 min, and lysates were incubated with anti-Myc monoclonal or anti-GFP polyclonal (Rockland, Gilbertsville, PA) antibodies for 3 h. The immunocomplexes were then recovered using 30 μL of Protein A/G Plus agarose (Santa Cruz Biotechnology, Santa Cruz, CA) and analyzed by immunoblotting.

Preparation of Recombinant Proteins. Glutathione *S*-transferase (GST) fusion proteins of various fragments of PRG and frabin were expressed in transformed *Escherichia coli* cells (BL 21). Cells were grown in 2YT medium at 37 °C to an A_{600} of ∼0.7, induced with 0.5 mM isopropyl 1-thiogalactopyranoside (Fisher Scientific, Fair Lawn, NJ), and grown for 3 h.

Subsequently, cells were pelleted and lysed by sonication in STE [20 mM Tris-HCl (pH 8.0), 150 mM NaCl, and 1 mM EDTA (pH 8.0)] containing 5 mM DTT, 2% Triton X-100, 1.5% Sarkosyl, 2 mg/mL lysozyme, 1 mM PMSF, 10 μg/mL leupeptin, 10 μg/mL aprotinin, and complete protease inhibitor cocktail tablets (Roche Diagnostics). The suspension was then centrifuged at 27000*g* (Sorvall SS-34 rotor) for 30 min at 4 °C. The supernatants were incubated with glutathione-Sepharose beads (GE Healthcare) for 2 h at 4 °C. Beads were washed thrice with lysis buffer. Following washes, the GST-fused proteins were eluted off the beads with buffer [50 mM Tris-HCl (pH 8.0) and 1 mM PMSF] containing 10 mM reduced glutathione (Sigma-Aldrich, St. Louis, MO). The eluted protein was subjected to dialysis in buffer containing 20 mM NaCl, 20 mM Tris-HCl (pH 8.0), and 2.5% glycerol. For F-actin bundling assays, proteins were cleaved off GST using Factor Xa Protease (New England Biolabs, Ipswich, MA); the degree of removal of GST was >90% routinely.

F-Actin Cosedimentation Assay. Purified GST-fused fragments were precleared by centrifugation at 200000*g* (TLA 100.2 rotor; Beckman Instruments, Palo Alto, CA) for 20 min at 4 °C to remove any aggregates, and the resultant supernatant was used for the experiment. The actin cosedimentation assay was conducted essentially as described by the manufacturer (Cytoskeleton, Inc., Denver, CO). Briefly, recombinant proteins were incubated with 40 μg of freshly polymerized actin (F-actin) for 30 min at room temperature. After incubation, the protein/F-actin solution was subjected to high-speed centrifugation (160000*g*) to pellet F-actin and protein bound to F-actin. The pellet fractions were solubilized in SDS sample buffer, the volume being equal to the initial incubation volume. Equivalent amounts of pellet and supernatant fractions were analyzed by SDS−PAGE followed by staining using Novex colloidal blue (Invitrogen, Carlsbad, CA). To quantify F-actin binding, increasing amounts of F-actin were incubated with recombinant proteins as mentioned in the figure legends. The samples were then centrifuged and analyzed as described above. The protein bands were quantified by densitometry using Quantity One analysis software (Bio-Rad, Hercules, CA).

Observation of Actin Bundles. The following recombinant proteins were used in this assay: GST, GST(541−605)PRG, GST(541−605,Δ25)PRG, (541−605)PRG, monomeric (541−605)PRG-FKBP, and dimeric (541−605)PRG-FKBP. In the case of (541−605)PRG and (541−605)PRG-FKBP, GST was removed by proteolytic cleavage. For inducible experiments, 25 μM (541−605)PRG-FKBP (lacking GST) was incubated without or with 25 μM AP20187 (Ariad Pharmaceuticals) at room temperature for 15 min to prepare monomeric or dimeric (541−605)PRG-FKBP, respectively. Using these 25 μM stocks, monomeric and dimeric forms of (541−605)PRG-FKBP were diluted and used in the assay at 5 and 10 μM. In all other cases, 7 μM recombinant protein was used.

Fluorescence observation of actin bundles was performed as described previously (*31*). Briefly, 1.2 μM freshly polymerized F-actin was incubated alone or with the recombinant proteins described above in F-buffer [25 mM Hepes (pH 7.5), 100 mM KCl, 0.2 mM $CaCl_2$, 2 mM $MgCl_2$, 2 mM EGTA, 0.2 mM ATP, and 1 mM DTT] for 30 min on ice. Next, F-actin was stained with phalloidin conjugated to Alexa 594 at a dilution of 1:100 for 15 min on ice. The mixture was then applied to poly-L-lysine-coated glass coverslips (BD Biosciences, Bedford, MA) and incubated for 20 min at room temperature. Adherent material was washed with F-buffer and observed using a 60× 1.4 NA oil immersion objective.

F-Actin Bundling Assay. (541−605)PRG-FKBP (25 μM) was dimerized using AP20187, as described above. The 25 μM stock of dimerized (541−605)PRG-FKBP was appropriately diluted (0.5−16 μM) and incubated with 1 μM F-actin in F-buffer at room temperature for 1 h. This mixture was then subjected to a low-speed centrifugation (10000*g*) for 30 min. Supernatant and pellet fractions were solubilized in SDS sample buffer and analyzed as described above.

Native Gel Electrophoresis. Native gel electrophoresis was performed in an 8% acrylamide gel prepared in 0.3 M Tris-HCl (pH 8.8). (541−605)PRG-FKBP (25 μM) was mixed with nondenaturing loading buffer [0.3 M Tris-HCl (pH 6.8), 50% glycerol, and 0.5% bromophenol blue], and the samples were loaded and run at 4 °C and 25 mA in 25 mM Tris base and 200 mM glycine. The gel was stained using Novex colloidal blue.

F-Actin Polymerization Assay. Pyrene-labeled actin (60% labeled) and the Arp2/3 complex were obtained from Cytoskeleton, Inc. The actin polymerization assay was performed as described previously (*32*). Briefly, pyrene-labeled actin was incubated in buffer containing 5 mM Tris-HCl (pH 7.5), 0.2 mM $CaCl_2$, and 0.2 mM ATP for 1 h on ice. Following incubation, residual F-actin was removed by centrifugation at 400000*g* for 1 h. Polymerization reaction mixtures contained either labeled actin (1 μM) used alone or in combination with the recombinant VCA domain (110 nM) of WAVE2 and the Arp2/3 complex (30 nM) as negative and positive controls, respectively. In addition, labeled actin (1 μM) was also incubated with monomeric and dimeric forms of (541−605)PRG-FKBP (1 μM). The actin polymerization reaction was initiated in polymerization buffer containing 100 mM Tris-HCl (pH 7.5), 10 mM $MgCl_2$, 500 mM KCl, 10 mM EGTA, and 0.2 mM ATP. Pyrene fluorescence was monitored continuously every 30 s with a spectrofluorimeter (Perkin-Elmer luminesecence spectrometer LS55) set at an excitation wavelength of 365 nm and an emission wavelength of 407 nm.

RESULTS

Prediction of an Actin-Binding Motif Shared by PRG and Frabin. Our previous investigation suggested that a nine-amino acid sequence, NIIQHFENN, consisting of amino acids 567−575, within the 561−585 actin-binding region is critical for the actin interaction of PRG (*29*). To examine the important elements of this sequence in more detail, here we have first compared the actin-binding region of human PRG to the similar region of the mouse and zebrafish PRG orthologs (Figure 1). Much of this region is highly conserved, even in zebrafish PRG, suggesting that actin binding ability has been retained in PRG across species. Consistent with this, a recent report showed colocalization with F-actin of the zebrafish PRG when expressed in HEK293 cells (*33*).

In addition, in our previous study we speculated that a similar actin-binding motif is present in frabin, a RhoGEF for Cdc42. It has been shown that frabin binds to actin through its 150 N-terminal amino acids (*34*). Although the minimal sequence for actin binding was not defined in frabin, it was reported that mutation of leucine at position 23 to arginine abolished binding to actin (*30*). A comparison of the amino acid sequence surrounding L^{23} of frabin with the actin-binding region of PRG identifies some similarity, showing that two hydrophobic

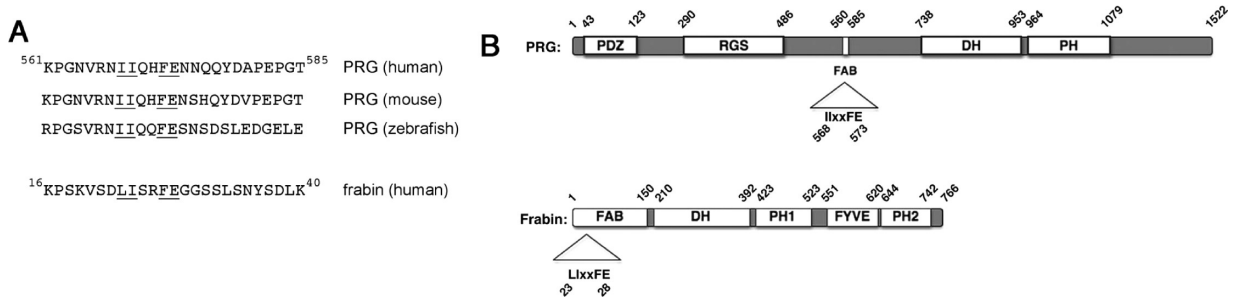

FIGURE 1: Actin-binding motif of PRG and frabin. (A) Amino acid sequence encompassing the predicted actin-binding motif in human PRG (amino acids 561−585) along with sequences in similar locations in the mouse and zebrafish PRG orthologs. In addition, the predicted actin-binding motif (amino acids 16−40) of frabin is shown. The underlined amino acids indicate similarities among PRG orthologs and frabin, and the underlined amino acids represent a minimal actin-binding motif, L/IIxxFE, defined in this report. (B) Locations of the actin-binding motif in the overall structure of PRG and frabin.

residues, leucine and/or isoleucine, an aromatic residue, phenylalanine, and an acidic residue, glutamic acid, are conserved among the PRG orthologs and human frabin (Figure 1). This sequence analysis thus suggests L/IIxxFE as a critical motif in the actin-binding domain of both PRG and frabin. The experiments described below confirm this prediction.

Subcellular Localization of PDZ-RhoGEF. In PRG, the stretch of nine amino acids, NIIQHFENN, at positions 567−575, plays a crtitical role in localization of the protein to the peri-PM region in 293T and COS-7 cells (*29*). To identify amino acids that are absolutely critical in binding to actin, we individually mutated each of these nine residues to alanine and examined PRG localization by immunofluorescence. PRG and its mutants containing an N-terminal Myc epitope tag were expressed in COS-7 cells; all PRG mutants exhibit similar expression levels (not shown). As observed earlier, wild-type (WT) PDZ-RhoGEF (Myc-PRG) displayed cytoplasmic as well as peri-PM localization (Figure 2a). In addition, Myc-PRG was also found to colocalize with cortical actin at the cell periphery (Figure 2b) as seen by staining for actin using fluorescently labeled phalloidin. Point mutants Myc(N567A)PRG (Figure 2c,d), Myc-(Q570A)PRG, Myc(H571A)PRG (Figure 2i−l), Myc(N574A)-PRG, and Myc(N575A)PRG (Figure 2q−t) displayed localization similar to that of Myc-PRG. These mutants were also observed to colocalize with cortical actin. On the other hand, mutants Myc(I568A)PRG, Myc(I569A)PRG (Figure 2e−h), Myc(F572A)PRG, and Myc(E573A)PRG (Figure 2m−p) exhibited a complete loss of peri-PM localization and failed to colocalize with actin. These observations suggest that four amino acids, isoleucines at positions 568 and 569, phenylalanine at position 572, and glutamic acid at position 573, play a critical role in the peri-PM localization of PRG in COS-7 cells.

Subcellular Localization of Frabin. As with PRG, we examined the potential actin-binding motif of frabin by individually mutating each of the nine amino acids in the DLISHFEGG sequence at positions 22−30 to alanine. Mutations were introduced into an N-terminal 150-amino acid region of frabin fused to GFP that was previously shown to bind actin (*30*), and the subcellular distribution of the mutants was detected using fluorescence microscopy; all frabin proteins exhibited similar expression levels (not shown).

Frabin(1−150)GFP when transiently transfected in COS-7 cells showed a strong colocalization with actin both at the cell periphery and within the cell as seen by staining for actin using a fluorescently labeled phalloidin (Figure 3a,b). Similarly, frabin-(1−150,D22A)GFP (Figure 3c,d), frabin(1−150,S25A)GFP, frabin(1−150,H26A)GFP (Figure 3i−l), frabin(1−150,G29A)-GFP, and frabin(1−150,G30A)GFP (Figure 3q−t) showed a strong colocalization with actin. Intriguingly, mutations that abolished colocalization with actin in similar positions of PRG also abolished frabin's colocalization with actin. Frabin(1−150, L23A)GFP, frabin(1−150,I24A)GFP (Figure 3e−h), frabin(1−150,F27A)GFP, and frabin(1−150,E28A)GFP (Figure 3m−p) displayed little or no colocalization with actin, and the subcellular distribution of these point mutants was identical to that of GFP alone (data not shown). Thus, individual mutation of L^{23}, I^{24}, F^{27}, and E^{28} caused a complete loss of colocalization of frabin with the actin cytoskeleton in COS-7 cells. PRG point mutants that resembled the frabin mutants also exhibited defective colocalization with the actin cytoskeleton (Figure 2). Taken together, these observations indicate the importance of these four conserved residues in localization of PRG and frabin to the actin cytoskeleton.

A Conserved Motif in PRG and Frabin Is Critical for Co-Immunoprecipitation with Actin. Next we performed co-immunoprecipitation assays to test the importance of these residues in the interaction of PRG and frabin with actin. COS-7 cells were transiently transfected with the wild type and point mutants of PRG, frabin, or frabin(1−150)GFP. Overexpressed proteins were immunoprecipitated, and immunoblots were probed with anti-actin antibody to assess co-immunoprecipitation.

As shown in Figure 4A (top panel), actin co-immunoprecipitates with Myc-PRG. Mutants Myc(N567A)PRG, Myc(Q570A)-PRG, Myc(H571A)PRG, Myc(N574A)PRG, and Myc(N575A)-PRG that colocalize with actin were also able to efficiently co-immunoprecipitate with actin. However, Myc(I568A)PRG, Myc-(I569A)PRG, Myc(F572A)PRG, and Myc(E573A)PRG, which failed to colocalize with actin, show little or no co-immunoprecipitation with actin.

As expected, actin co-immunoprecipitated with full-length frabin, whereas little or no co-immunoprecipitation of actin was observed with empty vector or GFP alone (Figure 4B,C). Frabin(1−150)GFP which strongly colocalizes with actin as observed by immunofluorescence (Figure 3) also efficiently co-immunoprecipitated with actin (Figure 4C); in addition, point mutants frabin(1−150,D22A)GFP, frabin(1−150,S25A)GFP, frabin(1−150,H26A)GFP, frabin(1−150,G29A)GFP, and frabin-(1−150,G30A)GFP, all of which colocalize with actin (Figure 3), strongly interact with actin as observed by co-immunoprecipitation. However, mutants frabin(1−150,L23A)GFP, frabin(1−150, I24A)GFP, frabin(1−150,F27A)GFP, and frabin(1−150,E28A)-GFP fail to co-immunoprecitate with actin, suggesting the

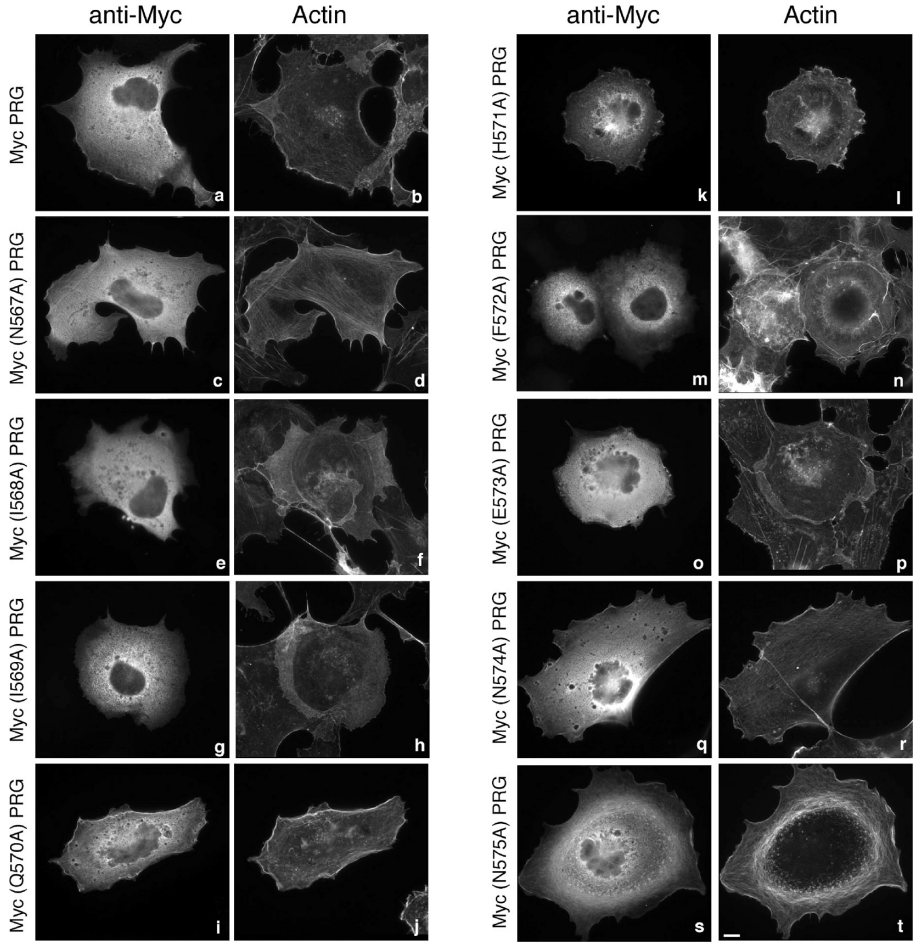

FIGURE 2: Subcellular localization of PRG and mutants. COS-7 cells were transfected with 1 μg of an expression vector encoding Myc epitope-tagged PRG (a and b), Myc(N567A)PRG (c and d), Myc(I568A)PRG (e and f), Myc(I569A)PRG (g and h), Myc(Q570A)PRG (i and j), Myc(H571A)PRG (k and l), Myc(F572A)PRG (m and n), Myc(E573A)PRG (o and p), Myc(N574A)PRG (q and r), or Myc(N575A)PRG (s and t). Twenty-four hours post-transfection, cells were fixed and subjected to immunofluorescence microscopy as described in Materials and Methods. Expressed proteins were detected with an anti-Myc 9E10 antibody (a, c, e, g, i, k, m, o, q, and s) followed by Alexa 594 conjugated to an anti-mouse antibody. Actin was visualized in the same cells by costaining with Alexa 488 conjugated to phalloidin (b, d, f, h, j, l, n, p, r, and t). The bar is 10 μm. Images shown are single cells representative of at least five separate experiments in which more than 50 cells were viewed in each experiment. Note that wild-type PRG (a) and unaffected PRG mutants (c, i, k, q, and s) show a modest colocalization with F-actin at the cell periphery, whereas I568A, I569A, F572A, and E573A mutants of PRG (e, g, m, and o, respectively) reproducibly display a complete loss of staining at the cell periphery.

importance of these residues for interaction with actin. Thus, in both PRG and frabin, identical residues play a role in interaction with actin.

PRG Binds to F-Actin in Vitro. So far, we have shown that PRG interacts with actin in cells. However, it has not been demonstrated whether PRG directly binds to actin through this 25-amino acid region or if instead binding to actin is mediated via other interacting proteins. To address this, we performed an actin cosedimentation assay using purified proteins. GST-fused PRG comprising amino acids 541−605 with or without the 25-amino acid actin-binding domain was used for this experiment. In addition, point mutants of the key residues that were observed earlier to be involved in interaction with actin (Figures 2 and 4) were also made in the context of the PRG(541−605)GST fusion protein. Recombinant proteins (2 μM) were incubated with freshly polymerized F-actin (20 μM), and the ability of proteins to cosediment with actin was examined (Figure 5). Cosedimentation with F-actin in the pellet fraction (P) following a high-speed centrifugation indicates binding to F-actin, while separation into the soluble fraction (S) indicates no interaction with F-actin. As shown in Figure 5A, GST alone partitioned entirely in the soluble fraction both in the absence and in the presence of F-actin (Figure 5A, lane 1). GST(541−605)PRG (Figure 5A, lane 2) was entirely in the soluble fraction without F-actin. However, in the presence of F-actin, GST(541−605)PRG partitioned to the F-actin-bound pellet fraction, demonstrating for the first time direct binding to actin of PRG's actin-binding domain. Similarly, GST(541−605,N574A)PRG (Figure 5A, lane 7) also cosedimented with F-actin in the pellet fraction. In contrast, GST(541−605, I568A)PRG (Figure 5A, lane 3) and GST(541−605,I569A)PRG (Figure 5A, lane 4) exhibited impaired partitioning to the F-actin-bound pellet fraction, and GST(541−605,F572A)PRG (Figure 5A, lane 5) and GST(541−605,E573A)PRG (Figure 5A, lane 6) displayed very little partitioning to the F-actin-bound pellet fractions, suggesting the importance of these residues in F-actin binding in vitro. GST(541−605,Δ25)PRG (Figure 5A, lane 8), which lacks the actin-binding domain, failed to cosediment with actin and was always in the soluble fraction regardless of the presence or absence of F-actin.

To examine more closely the binding of PRG to F-actin, we first tested dose-dependent binding of GST(541−605)PRG with actin. A cosedimentation assay was performed in which 3 μM

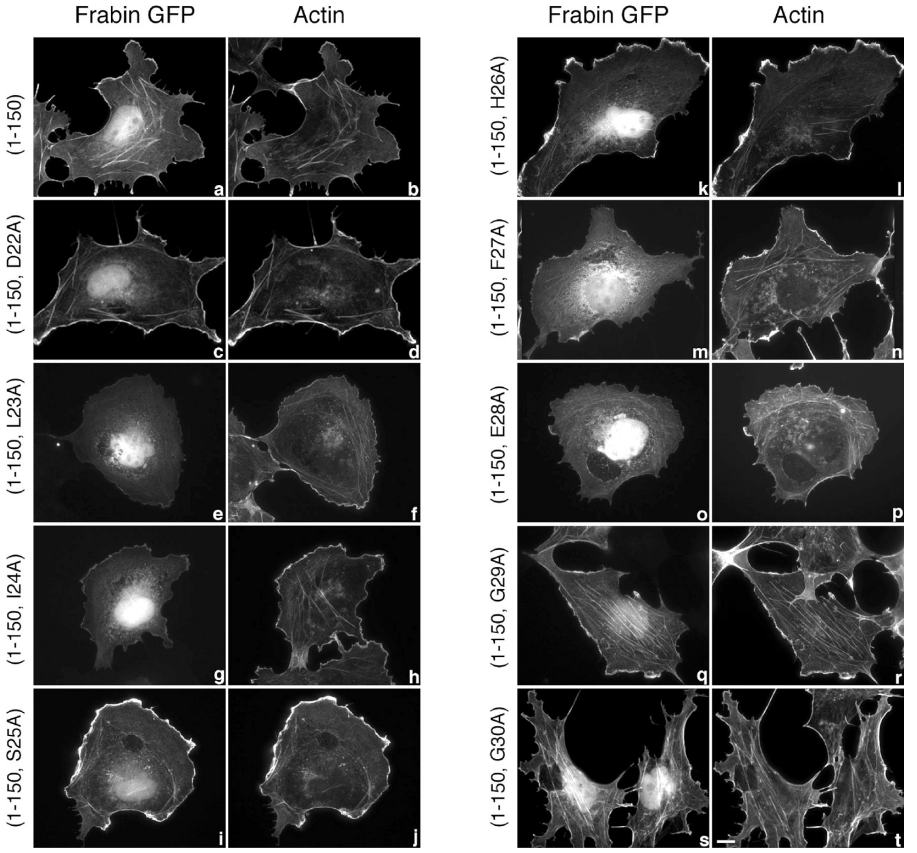

FIGURE 3: Subcellular localization of frabin mutants. COS-7 cells were transiently transfected with 1 μg expression vectors encoding GFP-tagged frabin mutants, frabin(1−150) (a and b), frabin(1−150,D22A) (c and d), frabin(1−150,L23A) (e and f), frabin(1−150,I24A) (g and h), frabin(1−150,S25A) (i and j), frabin(1−150,H26A) (k and l), frabin(1−150,F27A) (m and n), frabin(1−150,E28A) (o and p), frabin(1−150,G29A) (q and r), and frabin(1−150,G30A) (s and t). Expressed proteins were visualized by GFP fluorescence (a, c, e, g, i, k, m, o, q, and s), and actin was visualized (b, d, f, h, j, l, n, p, r, and t) in the same cells by staining with Alexa 594 conjugated to phalloidin. The bar is 10 μm. Images shown are single cells representative of at least five separate experiments in which more than 50 cells were viewed in each experiment. Note that frabin(1−150) (a) and unaffected frabin(1−150) mutants (c, i, k, q, and s) exhibit an intense GFP signal at the cell periphery and at intracellular stress fibers that colocalizes with F-actin, whereas L23A, I24A, F27A, and E28A frabin(1−150) (e, g, m, and o, respectively) reproducibly display a weak GFP signal at the cell periphery. The weak signal at the cell periphery observed with the four frabin mutants (e, g, m, and o) is identical to the background signal of GFP alone.

recombinant protein was incubated with variable concentrations of F-actin (0.2−20 μM). We observed that GST(541−605)PRG cosedimented with F-actin in a concentration-dependent manner, reaching saturation at approximately 5 μM F-actin. At this F-actin concentration, approximately 75% of GST(541−605)PRG was bound to actin as determined by densitometric analysis (Figure 5B, i). From the resulting binding curve, we also estimated that GST(541−605)PRG bound to F-actin with an apparent dissociation constant (K_d) of ~1 μM. However, in the case of GST(541−605,I568A)PRG, GST(541−605,I569A)PRG, GST(541−605,F572A)PRG, and GST(541−605,E573A)PRG (Figures 5B, ii and iii, and not shown), only ~25% of the protein bound to F-actin at 5 μM, confirming that these mutants were defective in binding to actin. In the case of GST(541−605,Δ25)PRG (Figure 5B, iv), only 10% of the protein bound to actin at 5 μM, clearly indicating the role of the 25-amino acid domain between amino acids 561 and 585 of PRG in binding to actin in vitro. Similar to GST(541−605)PRG, GST-frabin mutants were tested for binding to actin in vitro. While GST(1−150)frabin efficiently cosedimented with F-actin as described previously (*30*), GST(1−150,L23A)frabin, GST(1−150,I24A)-frabin, GST(1−150,F27A)frabin, and GST(1−150,E28A)frabin displayed defective binding to actin in vitro (data not shown). Thus, data obtained from cosedimentation assays demonstrate the novel finding that PRG binds to F-actin in vitro and that the L/IIxxFE sequence is critical for actin binding of both PRG and frabin.

The Dimeric PRG Actin-Binding Domain Induces Bundling of F-Actin in Vitro. Next, we asked whether the PRG actin-binding domain could effect changes in F-actin structure. Interestingly, the PRG actin-binding domain exhibited an actin bundling activity. Freshly polymerized F-actin was incubated with recombinant GST-tagged proteins; actin was stained with fluorescently labeled phalloidin, and actin filaments were visualized via fluorescence microscopy, using a previously described procedure (*31*). F-Actin formed a meshwork of filaments when observed in the absence of added recombinant protein (Figure 6A, a) or in the presence of GST (Figure 6A, b). However, incubation with GST(541−605)PRG induced thick F-actin bundles (Figure 6A, c); actin bundles were not formed when F-actin was incubated with GST(541−605,Δ25)PRG (Figure 6A, d). Thus, these experiments indicate that GST(541−605)PRG directly promotes actin bundling.

Actin bundling activity in a protein often requires either two independent F-actin-binding sites or oligomerization of a protein containing a single F-actin-binding site. Interestingly, frabin, which we show in this report to have an actin-binding motif similar to that of PRG, has been reported to cause bundling of

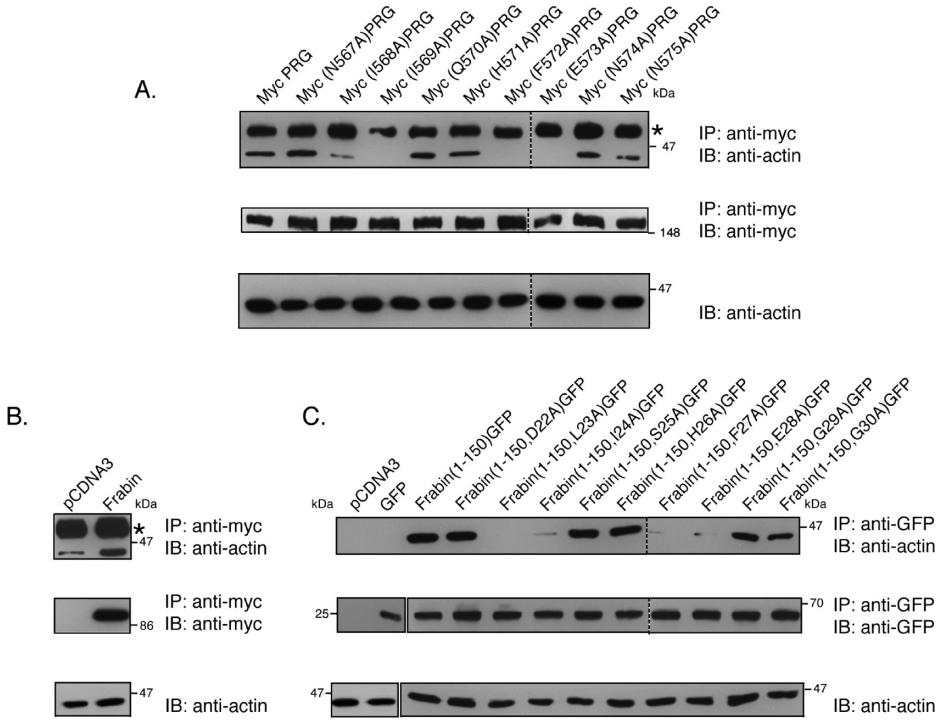

FIGURE 4: PRG and frabin co-immunoprecipitate with actin. (A) COS-7 cells were transiently transfected with 7 μg of an expression vector encoding PRG or the indicated mutants. PRG was immunoprecipitated from cell lysates with a mouse monoclonal anti-Myc antibody, and immunoprecipitates were analyzed by immunoblotting using an anti-actin mAb (top panel). Immunoprecipitation of the Myc-tagged PRG proteins was confirmed by immunoblotting of the immunoprecipitates using an anti-Myc antibody (middle panel). The presence of actin in the lysates was detected by immunoblotting using an anti-actin mAb (bottom panel). (B) COS-7 cells were transfected with 7 μg of empty vector or with expression plasmid for Myc-tagged full-length frabin. Cells were lysed, and lysates were subjected to immunoprecipitation with a monoclonal anti-Myc antibody. Immunoprecipitates were analyzed by immunoblotting using an anti-actin mAb (top panel) and an anti-Myc antibody (middle panel). Actin in the cell lysates was detected using an anti-actin mAb (bottom panel). (C) COS-7 cells were transiently transfected with 7 μg of empty vector, GFP alone, or the indicated GFP-tagged frabin mutants. Cell lysates were immunoprecipitated with a polyclonal anti-GFP antibody, and immunoprecipitates were probed for actin using an anti-actin mAb (top panel). Immunoprecipitation of GFP-tagged frabin constructs was confirmed by immunoblotting of immunoprecipitates using an anti-GFP antibody (middle panel), and the presence of actin in the cell lysates was confirmed with an anti-actin mAb (bottom panel). Asterisks indicate the antibody heavy chain that migrates slower than actin.

F-actin, although the mechanism is unclear (*34*). The 65-amino acid portion of PRG contained in GST(541−605)PRG likely contains only one actin-binding site because of its small size and our results which show that single mutations can abolish actin binding. GST is known to exist in solution as a dimer, and thus, GST(541−605)PRG would exist as a dimer. Thus, we hypothesized that the dimerization of (541−605)PRG is necessary for actin bundling. This proposal is particularly relevant since a recent report indicated that PRG forms dimers in cells (*22*).

To test this, GST was removed following a proteolytic cleavage, and the resulting (541−605)PRG was incubated with F-actin. Interestingly, F-actin bundling was no longer observed when (541−605)PRG was incubated with F-actin (Figure 6A, e). To further test the possibility that dimers of the actin-binding domain of PRG induce F-actin bundling, we took advantage of an inducible dimerization system in which the rapamycin binding protein FKBP is fused to the protein of interest and dimerization is induced by a dimerizing rapamycin analogue termed AP20187 (*35*). For this, we created GST(541−605)PRG-FKBP. GST was cleaved off, and the resultant (541−605)PRG-FKBP was first tested for its ability to cosediment with F-actin (Figure 6B). As expected, the protein was entirely in the soluble fraction in the absence of F-actin. In the presence of F-actin, the protein cosedimented with F-actin in the pellet fraction (Figure 6B), confirming the ability of (541−605)PRG-FKBP to bind F-actin. Next, (541−605)PRG-FKBP (25 μM) was treated with increasing concentrations of the dimerizer AP20187 (5−100 μM). A concentration-dependent shift in the mobility of the protein in a native gel (Figure 6C) indicated the AP20187-dependent dimerization of (541−605)PRG-FKBP. (541−605)-PRG-FKBP was then tested for its ability to induce bundling of F-actin. In the absence of AP20187, 5 and 10 μM monomeric (541−605)PRG-FKBP failed to cause bundling of F-actin (Figure 6D, top panel). In contrast, (541−605)PRG-FKBP which was dimerized using AP20187 induced F-actin bundling (Figure 6D, bottom panel). Incubation of 1.2 μM F-actin with 5 μM dimerized (541−605)PRG-FKBP caused thickening of F-actin (Figure 6D, b). Well-organized F-actin bundles were observed (Figure 6D, d) when 1.2 μM F-actin was incubated with 10 μM dimerized (541−605)PRG-FKBP, indicating a dose-dependent ability to induce actin bundling.

To further study actin bundling by dimerized (541−605)PRG-FKBP, a low-speed centrifugation assay was performed (*31*). Briefly, 1 μM F-actin was incubated with either monomeric or dimerized (541−605)PRG at room temperature for 1 h. The protein−F-actin complex was then subjected to a low-speed centrifugation (10000*g*). Bundled F-actin is found in the pellet (P) fraction, while unbundled F-actin remains in the soluble (S) fraction. In the absence of the dimerizer AP20187, (541−605)PRG promoted a partial shift of F-actin into the pellet fraction (Figure 6E). However, dimerization of (541−605)PRG-FKBP and incubation with F-actin resulted in a strong shift of F-actin into the pellet fraction, consistent with the ability of dimerized (541−605)PRG-FKBP to promote actin bundling.

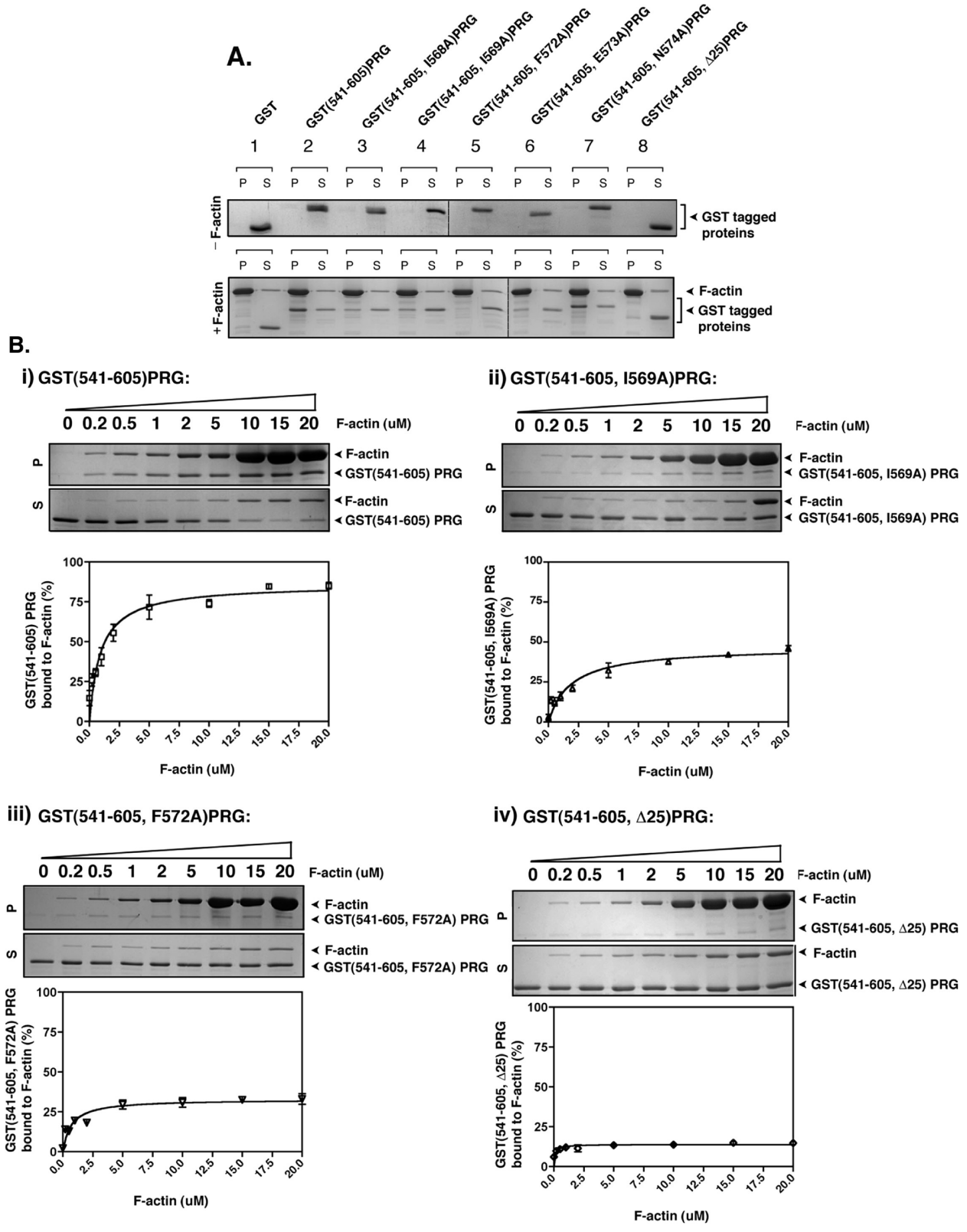

FIGURE 5: PRG binds to F-actin in vitro. (A) The indicated recombinant protein (2 μg) was incubated with or without 40 μg of freshly polymerized F-actin at room temperature for 30 min and then centrifuged at 160000*g* for 90 min. Equal aliquots of resuspended pellet (P) and supernatant (S) were analyzed via SDS−PAGE and colloidal blue staining. (B) Quantification of F-actin binding activity of recombinant PRG mutants, GST(541−605)PRG (i), GST(541−605,I569A)PRG (ii), GST(541−605,F572A)PRG, and (iv) GST(541−605,Δ25)PRG. The indicated mutants of PRG (3 μM) were incubated with variable concentrations of F-actin (0.2−20 μM) and cosedimented at 160000*g* for 90 min. Equal aliquots of resuspended pellet (P) and supernatant (S) were analyzed by SDS−PAGE and colloidal blue staining (top panels), and the bands were quantified by densitometry. The percentage of F-actin-bound PRG mutants was calculated as the percentage recovered in the pellet (P) over the total protein (S + P). The graphs represent the means ± the standard deviation of three independent experiments.

Moreover, dimerized (541−605)PRG displayed a concentration-dependent actin bundling activity (Figure 6F,G). AP20187 alone, in the absence of (541−605)PRG-FKBP, did not cause bundling of actin (data not shown). From these results (Figure 6),

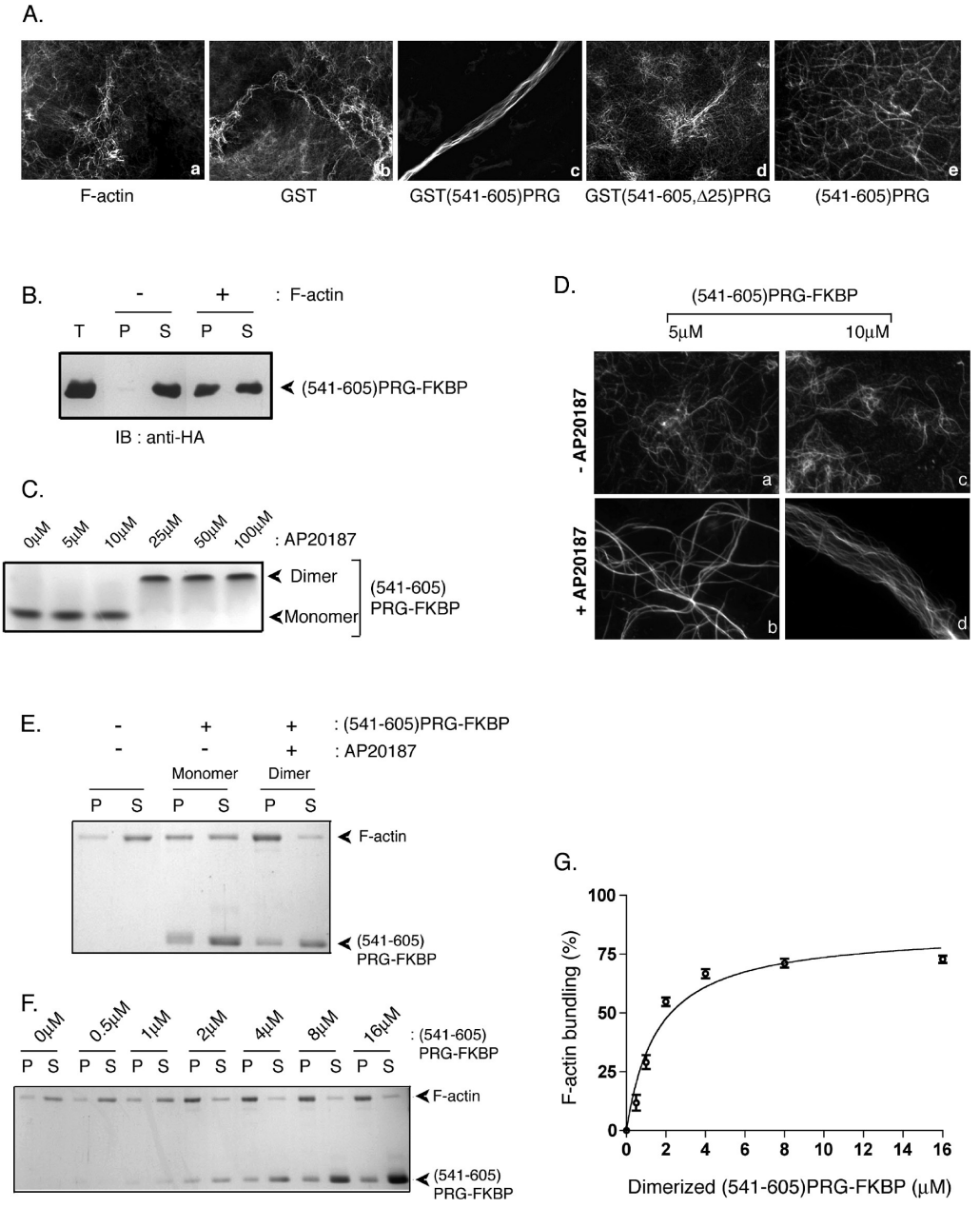

FIGURE 6: PRG induces F-actin bundling in vitro. (A) F-Actin (1.2 μM) was incubated alone (a) or with 7 μM GST (b), GST(541−605)PRG (c), GST(541−605,Δ25)PRG (d), or (541−605)PRG from which GST was removed by proteolysis (e) for 30 min on ice. After being stained with phalloidin, actin filaments and bundles were observed by fluorescence microscopy. (B) (541−605)PRG-FKBP (GST removed by proteolysis) incubated with or without freshly polymerized actin was subjected to a high-speed cosedimentation assay at 160000*g* for 90 min. Equal aliquots of pellet and supernatant fractions along with total protein (T) were immunoblotted using an anti-HA antibody to detect (541−605)PRG-FKBP. (C) (541−605)PRG-FKBP (25 μM) was incubated with variable concentrations (5−100 μM) of AP20187 for 15 min at room temperature. Samples were subjected to native gel electrophoresis followed by colloidal blue staining. (D) (541−605)PRG-FKBP (5 and 10 μM) treated without (a and c) and with (b and d) AP20187 was incubated with 1.2 μM freshly polymerized F-actin. Following incubation, F-actin was stained with phalloidin and observed by fluorescence microscopy. (E) Monomeric or dimeric (541−605)PRG-FKBP (2 μM) was incubated with 1 μM freshly polymerized F-actin, and samples were centrifuged at 10000*g* for 30 min. Equal amounts of pellet (P) and supernatant (S) fractions were resolved by SDS−PAGE and stained using colloidal blue. (F) To quantitate the F-actin bundling activity of dimerized (541−605)PRG-FKBP, 0, 0.5, 1, 2, 4, 8, or 16 μM dimerized (541−605)PRG-FKBP was incubated with 1 μM F-actin. Samples were then centrifuged at 10000*g*. Equal amounts of pellet (P) and supernatant (S) fractions were run via SDS−PAGE and stained with colloidal blue. (G) F-Actin in the 10000*g* pellet fraction in panel F was quantitated using densitometry. The percentages of F-actin bundled using different amounts of dimerized (541−605)PRG-FKBP were calculated as the percentages recovered in the pellet (P) over total protein (S + P). The data represent the means ± the standard deviation of three independent experiments.

we conclude that (541−605)PRG-FKBP causes F-actin bundling in vitro, and this is regulated by the protein's ability to dimerize.

Lastly, we examined the effect of recombinant (541−605)-PRG on actin polymerization. Using a well-described pyrene-labeled actin assay (*32*, *36*), neither monomeric nor dimeric (541−605)PRG was able to increase the rate of actin polymerization (Figure S1 of the Supporting Information). However, the positive control of the VCA domain of WAVE2 with Arp2/3 displayed the expected dramatic increase in the level of actin polymerization. Thus, we conclude that the actin-binding domain of PRG alone does not affect polymerization of F-actin in vitro.

DISCUSSION

This report defines a novel actin-binding motif in PDZ-RhoGEF (PRG) and shows that this motif is responsible for directly binding F-actin in vitro and localizing PRG to the actin cytoskeleton in cells. In addition, we demonstrate that a similar actin-binding motif is found in the RhoGEF frabin. Extensive mutagenesis defines the consensus sequence for this actin-binding motif as L/IIxxFE. Lastly, we show that the PRG actin-binding region can promote the bundling of actin in vitro in a dimerization-dependent manner.

Our previous work defined a 25-amino acid region at positions 561−585 in PRG that was necessary and sufficient for actin interaction and further indicated the importance of a nine-amino acid stretch from position 567 to 575 of the NIIQHFENN sequence (*29*). Because this sequence did not appear to match any known actin-binding sequence modules (*37*), it was important to further define the critical amino acids in the actin-binding sequence of PRG. Each amino acid in the 567−575 sequence was individually substituted with alanine in full-length PRG. Individual mutation of isoleucine 568, isoleucine 569, phenylalanine 572, and glutamic acid 573 was sufficient to disrupt PRG's colocalization and co-immunoprecipitation with actin (Figures 2 and 4). Mutation of each of the other residues in the 567−575 sequence had no effect on localization or co-immunoprecipitation. Additionally, mutation of isoleucine 568, isoleucine 569, phenylalanine 572, and glutamic acid 573 in the context of GST(541−605)PRG inhibited direct binding to F-actin. Thus, these results define IIxxFE as the critical actin-binding motif in PRG.

Strikingly, visual inspection of the RhoGEF frabin revealed a sequence with identity to the actin-binding motif of PRG. Previously, actin binding was shown to exist in a fragment of frabin consisting of the N-terminal amino acids 1−150. Although an actin-binding sequence within the region of amino acids 1−150 was not defined, a mutation of leucine 23 to arginine disrupted actin binding and provided a clue that leucine 23 was likely part of an actin-binding sequence. The sequence surrounding leucine 23 in frabin is DLISHFEGG (amino acids 22−30), and thus, we tested whether frabin utilized similar amino acids for actin binding as does PRG by individually mutating each residue in the 22−30 amino acid sequence. Consistent with the results for PRG, mutation of leucine 23, isoleucine 24, phenylalanine 27, and glutamic acid 28 abrogated the ability of frabin residues 1−150 to colocalize with actin in cells, co-immunoprecipitate with actin, and directly bind to actin (Figures 3 and 4, and data not shown). Mutation of each of the other residues in the 22−30 sequence did not disrupt frabin localization or interaction with actin. Thus, these experiments reveal the LIxxFE sequence as a critical actin-binding motif in frabin. Taken together, results presented here have defined for the first time the actin-binding motifs of PRG and frabin. Importantly, these results show that both PRG and frabin utilize almost identical amino acids for binding actin. Thus, we identify the L/IIxxFE sequence as a novel actin-binding motif.

Interestingly, this actin-binding motif may be more widespread. Recently, a 17-amino acid peptide from the yeast protein Abp140 was shown to possess actin binding activity (*38*). Inspection of the peptide sequence, MGVADLIKKFESISKEE, reveals that it also contains the consensus motif LIxxFE. Although it was suggested that the Abp140 actin-binding sequence is not found in higher eukaryotes (*38*), our results suggest that mammalian proteins, such as PRG and frabin, utilize the same actin-binding motif and thus may bind actin in a manner similar to that of the Abp140 peptide. However, it remains to be demonstrated that the LIxxFE amino acids play a critical role in Abp140 actin binding. It will be interesting to test whether PRG and frabin compete with the Abp140 peptide for actin binding. Furthermore, a motif search revealed that the L/IIxxFE sequence is found in numerous proteins. Many of these proteins have no known interaction with actin. A future challenge will be to identify the proteins in which the presence of the L/IIxxFE motif represents a novel actin binding function.

In addition to defining a novel actin-binding motif, our results indicate that the PRG actin-binding region, when dimerized, is able to induce the bundling of F-actin. Using two assays for in vitro F-actin bundling, fluorescence microscopy and low-speed centrifugation, we demonstrated that the actin bundling activity of the purified actin-binding region of PRG depended on dimerization (Figure 6). Specifically, GST is known to form dimers, and consequently, removal of GST from GST(541−605)PRG abolished the actin bundling activity of (541−605)PRG. In addition, we used an inducible homodimerization system to show that dimeric (541−605)-PRG-FKBP induced actin bundling whereas monomeric (541−605)PRG-FKBP did not. Intriguingly, PRG and the other RGS-RhoGEFs, LARG and p115-RhoGEF, have been shown to exist as dimers, or possibly higher-order oligomers, in cells (*22*, *23*, *39*, *40*). Thus, we can speculate that PRG may affect the structure of the actin cytoskeleton in cells in a manner independent of or synergistic with its ability to activate Rho. Future studies will be needed to evaluate this proposal. Interestingly, frabin has been shown to also possess actin bundling activity (*34*). It has been suggested that frabin can directly reorganize a cell's actin cytoskeleton in a manner independent of activation of its cognate small GTPase Cdc42, and this actin bundling activity of frabin may thus play a role in the generation of F-actin bundles in filopodia (*34*, *41*). Other signaling proteins, including Ca^{2+}/calmodulin-dependent kinase II (CaMKII) (*42*−*44*), have been shown recently to have unexpected roles in bundling or stabilizing F-actin independent of their well-characterized enzyme activity.

The precise functional significance of actin binding and/or bundling by PRG remains to be determined. Actin binding is unique for PRG among the RGS-RhoGEFs. LARG and p115RhoGEF do not contain the actin-binding motif, and they do not localize to the actin cytoskeleton. Interestingly, the IIxxFE motif is also found in zebrafish PRG (Figure 1), and indeed, zebrafish PRG colocalizes with F-actin when expressed in HEK293 cells (*33*). Such conservation of the actin-binding motif suggests an evolutionarily retained function for actin binding by PRG. Previous work showed that PRG mutants that fail to interact with actin exhibited enhanced Rho-dependent signaling compared to that of wild-type PRG upon expression in HEK293 or Neuro2A cells, suggesting that actin binding may decrease PRG signaling function (*29*). However, the importance of actin binding by PRG remains to be addressed in a more physiological response; it will be interesting to define the role of the actin-binding domain in zebrafish PRG's role in developmental processes involving ciliated epithelia. A fuller understanding of the receptor-dependent responses for which PRG is an integral component will be necessary to unravel the importance of actin binding by PRG.

ACKNOWLEDGMENT

We thank Dr. Raja Bhattacharyya and Roshanak Irannejad for critically reading the manuscript, Dr. Yoshimi Takai for providing frabin cDNA, Dr. Natalia Zhukovskaya for help with actin fluorescence measurements and providing the purified VCA domain of WAVE2, and Dr. Dong Soo Kang, Matthew Martz, and Amrita Dawn for valuable experimental advice.

SUPPORTING INFORMATION AVAILABLE

A figure showing an actin polymerization assay. This material is available free of charge via the Internet at http://pubs.acs.org.

REFERENCES

1. Wennerberg, K., Rossman, K. L., and Der, C. J. (2005) The Ras superfamily at a glance. *J. Cell Sci. 118*, 843–846.
2. Bustelo, X. R., Sauzeau, V., and Berenjeno, I. M. (2007) GTP-binding proteins of the Rho/Rac family: Regulation, effectors and functions in vivo. *BioEssays 29*, 356–370.
3. Ridley, A. J., and Hall, A. (1992) The small GTP-binding protein rho regulates the assembly of focal adhesions and actin stress fibers in response to growth factors. *Cell 70*, 389–399.
4. Ridley, A. J., Paterson, H. F., Johnston, C. L., Diekmann, D., and Hall, A. (1992) The small GTP-binding protein rac regulates growth factor-induced membrane ruffling. *Cell 70*, 401–410.
5. Nobes, C. D., and Hall, A. (1995) Rho, rac, and cdc42 GTPases regulate the assembly of multimolecular focal complexes associated with actin stress fibers, lamellipodia, and filopodia. *Cell 81*, 53–62.
6. Jaffe, A. B., and Hall, A. (2005) Rho GTPases: Biochemistry and biology. *Annu. Rev. Cell Dev. Biol. 21*, 247–269.
7. Buchsbaum, R. J. (2007) Rho activation at a glance. *J. Cell Sci. 120*, 1149–1152.
8. Sternweis, P. C., Carter, A. M., Chen, Z., Danesh, S. M., Hsiung, Y. F., and Singer, W. D. (2007) Regulation of rho guanine nucleotide exchange factors by G proteins. *Adv. Protein Chem. 74*, 189–228.
9. Rossman, K. L., Der, C. J., and Sondek, J. (2005) GEF means go: Turning on RHO GTPases with guanine nucleotide-exchange factors. *Nat. Rev. Mol. Cell Biol. 6*, 167–180.
10. Hart, M. J., Sharma, S., elMasry, N., Qiu, R. G., McCabe, P., Polakis, P., and Bollag, G. (1996) Identification of a novel guanine nucleotide exchange factor for the Rho GTPase. *J. Biol. Chem. 271*, 25452–25458.
11. Rumenapp, U., Blomquist, A., Schworer, G., Schablowski, H., Psoma, A., and Jakobs, K. H. (1999) Rho-specific binding and guanine nucleotide exchange catalysis by KIAA0380, a Db1 family member. *FEBS Lett. 459*, 313–318.
12. Togashi, H., Nagata, K., Takagishi, M., Saitoh, N., and Inagaki, M. (2000) Functions of a Rho-specific guanine nucleotide exchange factor in neurite retraction: Possible role of a proline-rich motif of KIAA0380 in localization. *J. Biol. Chem. 275*, 29570–29578.
13. Reuther, G. W., Lambert, Q. T., Booden, M. A., Wennerberg, K., Becknell, B., Marcucci, G., Sondek, J., Caligiuri, M. A., and Der, C. J. (2001) Leukemia-associated Rho guanine nucleotide exchange factor, a Dbl family protein found mutated in leukemia, causes transformation by activation of RhoA. *J. Biol. Chem. 276*, 27145–27151.
14. Taya, S., Inagaki, N., Sengiku, H., Makino, H., Iwamatsu, A., Urakawa, I., Nagao, K., Kataoka, S., and Kaibuchi, K. (2001) Direct interaction of insulin-like growth factor-1 receptor with leukemia-associated RhoGEF. *J. Cell Biol. 155*, 809–820.
15. Aurandt, J., Vikis, H. G., Gutkind, J. S., Ahn, N., and Guan, K. L. (2002) The semaphorin receptor plexin-B1 signals through a direct interaction with the Rho-specific nucleotide exchange factor, LARG. *Proc. Natl. Acad. Sci. U.S.A. 99*, 12085–12090.
16. Driessens, M. H., Olivo, C., Nagata, K., Inagaki, M., and Collard, J. G. (2002) B plexins activate Rho through PDZ-RhoGEF. *FEBS Lett. 529*, 168–172.
17. Hirotani, M., Ohoka, Y., Yamamoto, T., Nirasawa, H., Furuyama, T., Kogo, M., Matsuya, T., and Inagaki, S. (2002) Interaction of plexin-B1 with PDZ domain-containing Rho guanine nucleotide exchange factors. *Biochem. Biophys. Res. Commun. 297*, 32–37.
18. Yamada, T., Ohoka, Y., Kogo, M., and Inagaki, S. (2005) Physical and functional interactions of the lysophosphatidic acid receptors with PDZ domain-containing Rho guanine nucleotide exchange factors (RhoGEFs). *J. Biol. Chem. 280*, 19358–19363.
19. Longhurst, D. M., Watanabe, M., Rothstein, J. D., and Jackson, M. (2006) Interaction of PDZRhoGEF with microtubule-associated protein 1 light chains: Link between microtubules, actin cytoskeleton, and neuronal polarity. *J. Biol. Chem. 281*, 12030–12040.
20. Chikumi, H., Fukuhara, S., and Gutkind, J. S. (2002) Regulation of G protein-linked guanine nucleotide exchange factors for Rho, PDZ-RhoGEF, and LARG by tyrosine phosphorylation: Evidence of a role for focal adhesion kinase. *J. Biol. Chem. 277*, 12463–12473.
21. Iwanicki, M. P., Vomastek, T., Tilghman, R. W., Martin, K. H., Banerjee, J., Wedegaertner, P. B., and Parsons, J. T. (2008) FAK, PDZ-RhoGEF and ROCKII cooperate to regulate adhesion movement and trailing-edge retraction in fibroblasts. *J. Cell Sci. 121*, 895–905.
22. Chikumi, H., Barac, A., Behbahani, B., Gao, Y., Teramoto, H., Zheng, Y., and Gutkind, J. S. (2004) Homo- and hetero-oligomerization of PDZ-RhoGEF, LARG and p115RhoGEF by their C-terminal region regulates their in vivo Rho GEF activity and transforming potential. *Oncogene 23*, 233–240.
23. Eisenhaure, T. M., Francis, S. A., Willison, L. D., Coughlin, S. R., and Lerner, D. J. (2003) The Rho guanine nucleotide exchange factor Lsc homo-oligomerizes and is negatively regulated through domains in its carboxyl terminus that are absent in novel splenic isoforms. *J. Biol. Chem. 278*, 30975–30984.
24. Hart, M. J., Jiang, X., Kozasa, T., Roscoe, W., Singer, W. D., Gilman, A. G., Sternweis, P. C., and Bollag, G. (1998) Direct stimulation of the guanine nucleotide exchange activity of p115 RhoGEF by Gα13. *Science 280*, 2112–2114.
25. Wells, C. D., Liu, M. Y., Jackson, M., Gutowski, S., Sternweis, P. M., Rothstein, J. D., Kozasa, T., and Sternweis, P. C. (2002) Mechanisms for reversible regulation between G13 and Rho exchange factors. *J. Biol. Chem. 277*, 1174–1181.
26. Suzuki, N., Nakamura, S., Mano, H., and Kozasa, T. (2003) Gα12 activates Rho GTPase through tyrosine-phosphorylated leukemia-associated RhoGEF. *Proc. Natl. Acad. Sci. U.S.A. 100*, 733–738.
27. Hart, M. J., Roscoe, W., and Bollag, G. (2000) Activation of Rho GEF activity by Gα13. *Methods Enzymol. 325*, 61–71.
28. Fukuhara, S., Murga, C., Zohar, M., Igishi, T., and Gutkind, J. S. (1999) A novel PDZ domain containing guanine nucleotide exchange factor links heterotrimeric G proteins to Rho. *J. Biol. Chem. 274*, 5868–5879.
29. Banerjee, J., and Wedegaertner, P. B. (2004) Identification of a novel sequence in PDZ-RhoGEF that mediates interaction with the actin cytoskeleton. *Mol. Biol. Cell 15*, 1760–1775.
30. Ikeda, W., Nakanishi, H., Tanaka, Y., Tachibana, K., and Takai, Y. (2001) Cooperation of Cdc42 small G protein-activating and actin filament-binding activities of frabin in microspike formation. *Oncogene 20*, 3457–3463.
31. Yamagishi, A., Masuda, M., Ohki, T., Onishi, H., and Mochizuki, N. (2004) A novel actin bundling/filopodium-forming domain conserved in insulin receptor tyrosine kinase substrate p53 and missing in metastasis protein. *J. Biol. Chem. 279*, 14929–14936.
32. Kim, Y., Sung, J. Y., Ceglia, I., Lee, K. W., Ahn, J. H., Halford, J. M., Kim, A. M., Kwak, S. P., Park, J. B., Ho Ryu, S., Schenck, A., Bardoni, B., Scott, J. D., Nairn, A. C., and Greengard, P. (2006) Phosphorylation of WAVE1 regulates actin polymerization and dendritic spine morphology. *Nature 442*, 814–817.
33. Panizzi, J. R., Jessen, J. R., Drummond, I. A., and Solnica-Krezel, L. (2007) New functions for a vertebrate Rho guanine nucleotide exchange factor in ciliated epithelia. *Development 134*, 921–931.
34. Obaishi, H., Nakanishi, H., Mandai, K., Satoh, K., Satoh, A., Takahashi, K., Miyahara, M., Nishioka, H., Takaishi, K., and Takai, Y. (1998) Frabin, a novel FGD1-related actin filament-binding protein capable of changing cell shape and activating c-Jun N-terminal kinase. *J. Biol. Chem. 273*, 18697–18700.
35. Spencer, D. M., Wandless, T. J., Schreiber, S. L., and Crabtree, G. R. (1993) Controlling signal transduction with synthetic ligands. *Science 262*, 1019–1024.
36. Cooper, J. A., and Pollard, T. D. (1982) Methods to measure actin polymerization. *Methods Enzymol. 85* (Part B), 182–210.
37. Maciver, S. K. (2004) http://www.bms.ed.ac.uk/research/others/smaciver/Encyclop/encycloABP.htm.
38. Riedl, J., Crevenna, A. H., Kessenbrock, K., Yu, J. H., Neukirchen, D., Bista, M., Bradke, F., Jenne, D., Holak, T. A., Werb, Z., Sixt, M., and Wedlich-Soldner, R. (2008) Lifeact: A versatile marker to visualize F-actin. *Nat. Methods 5*, 605–607.

39. Grabocka, E., and Wedegaertner, P. B. (2007) Disruption of oligomerization induces nucleocytoplasmic shuttling of leukemia-associated rho Guanine-nucleotide exchange factor. *Mol. Pharmacol. 72*, 993–1002.
40. Hu, J., Strauch, P., Rubtsov, A., Donovan, E. E., Pelanda, R., and Torres, R. M. (2008) Lsc activity is controlled by oligomerization and regulates integrin adhesion. *Mol. Immunol. 45*, 1825–1836.
41. Nakanishi, H., and Takai, Y. (2008) Frabin and other related Cdc42-specific guanine nucleotide exchange factors couple the actin cytoskeleton with the plasma membrane. *J. Cell. Mol. Med. 12*, 1169–1176.
42. Lin, Y. C., and Redmond, L. (2008) CaMKIIβ binding to stable F-actin in vivo regulates F-actin filament stability. *Proc. Natl. Acad. Sci. U.S.A. 105*, 15791–15796.
43. Okamoto, K., Narayanan, R., Lee, S. H., Murata, K., and Hayashi, Y. (2007) The role of CaMKII as an F-actin-bundling protein crucial for maintenance of dendritic spine structure. *Proc. Natl. Acad. Sci. U.S.A. 104*, 6418–6423.
44. Sanabria, H., Swulius, M. T., Kolodziej, S. J., Liu, J., and Waxham, M. N. (2009) βCaMKII regulates actin assembly and structure. *J. Biol. Chem. 284*, 9770–9780.